World Academy of Science, Engineering and Technology
International Journal of Mechanical and Mechatronics Engineering
Vol:6, No:8, 2012

Evaluation of Ultrasonic C-Scan Images by Fractal Dimension

S. Samanta, D. Datta, S. S. Gautam

***Abstract*—**In this paper, quantitative evaluation of ultrasonic C-scan images through estimation of their Fractal Dimension (FD) is discussed. Necessary algorithm for evaluation of FD of any 2-D digitized image is implemented by developing a computer code. For the evaluation purpose several C-scan images of the Kevlar composite impacted by high speed bullet and glass fibre composite having flaw in the form of inclusion is used. This analysis automatically differentiates a C-scan image showing distinct damage zone, from an image that contains no such damage.

***Keywords*—**C-scan, Impact, Fractal Dimension, Kevlar composite and Inclusion Flaw

I. Introduction

THE concept of fractals has been used extensively for graphical simulation of natural phenomena, study of image textures and analysis of material surfaces. Clouds, mountains, turbulent water, lightning and even music have all been shown to have a fractal form (Mandelbrot and Wallis [1]). Literature also indicates that fractal theory has been successfully implemented for characterizing statistical images. Such images are expected to have two important properties such as:

i) Each segment is statistically similar to all others.
ii) Segments at different scales are statistically indistinguishable and they often possess a remarkable invariance under changes of magnification.

In relation to ultrasonic application, the problem is to evaluate C-scan images in a quantitative way. Practically, FD of a surface corresponds quite close to our intuitive notion of roughness. A rough surface will have a smaller fractal dimension than that of a smooth surface. However the question of defining a fractal and how it is different from the usual Euclidean shape still remains. Mandelbrot [2] described fractal as a "shape made up of parts similar to the whole in someway." This property of self similarity or scaling is one of the central concepts of fractal geometry. It is closely connected with the intuitive notion of dimension. Pentland [3] showed that fractals can be effectively correlated with the perception of roughness in many situations. He extended the shape-form shading and shape from-texture methods to real surfaces. Lundhal et al. [4] demonstrated the use of fractal theory in analyzing X-ray medical images. Chen et al. [5] also applied the fractal concept to the classification and analysis of images obtained in X-ray medical imaging. Bhatt et al. [6] used fractal concept to analyze the quality of the reconstructed images in non medical areas.

S. Samanta and S. S. Gautam are with Mechanical Engineering Department, North Eastern Regional Institute of Science and Technology, Itanagar, India, [*suta_sama@yahoo.co.in].

D. Datta is with Mechanical Engineering Department, BESU, Shibpur, Howrah-711103,West Bengal, India.

They showed that the fractal dimension represented a reasonable quality index of the reconstructed images. Munshi et al. [7, 8] investigated the applicability of the fractal concept in the field of non destructive evaluation of real tomographic images. They applied fractal concept to analyze to tomograms obtained by an X-ray CT scanner.

In the present work ultrasonic C-scan is performed on different composite specimens by normal incidence immersion type pulse echo method. During scanning of flawed specimen relevant portion of the ultrasonic waveform is digitized at each point. Time domain features (Peak amplitude, Shannon entropy [9] etc) are extracted from digitized waveform at each point. C-scan images are generated by the systematic classification of the extracted feature values. These generated images are then utilized for quantitative evaluation through estimation of their Fractal Dimension.

II. Experimental Setup

The experimental set up comprises of (i) ballistic test set up for impacting the composite plates by bullets with recording of impact and exit velocities and (ii) the ultrasonic C-Scan setup for performing the immersion type ultrasonic C-scan. In the ballistic testing setup, the laminates are mounted on specially designed holders where two sides are clamped for rigid holding and placed in the line of fire of a 7.62 mm caliber military rifle. The impact energy is varied by adjusting the propellant mass in the ammunition. The impact and residual velocities are measured by the foil and counter method. A high speed video camera (operating at a rate of 10,000 frames per second) is also employed to observe the pre and post impact phenomena by taking pictures. The picture is stored in a PC for a frame-by-frame analysis.

Ultrasonic C-scan of an impacted composite laminate is done for making precise measurement of the variation of strength of the ultrasonic signal when the transducer is moved over a selected region around the zone of impact. This is accomplished through controlled and automated movement of the transducer in a plane parallel to the surface of the laminate. The facility comprises an immersion tank made of acrylic glass and a housing frame furnished with two lead screws in mutually perpendicular directions.

Two stepper motors drive the lead screws while a common nut, holding the probe holding device, moves linearly due to their rotation. The transducer, fitted in the probe holding device, can move along two mutually perpendicular directions in precise steps and is capable of scanning any predefined two-dimension region. The transducer is connected to an ultrasonic board (PCUS11 [10]) that acts as the pulsar, receiver and digitizer of the ultrasonic waveform. The board seamlessly interacts with the controlling software [11] that has the capability to condition, gate and zoom the digitized signal.

At each location, relevant portion of the waveform is digitized and is stored as an ASCII file for future post-processing.

III. Automated Imaging

In the present work an effort has been made for automatic generation of C-scan images for a set of given data using clustering technique. It is a way to create group of objects in such a way that the profiles of objects in the same group are very similar and those in different groups are quite distinct. Grouping of ultrasonic data is performed by implementation of UPGMAA algorithm [12] in a bid to ascertain their classes. Initially each object is treated as a separate group and merger of those groups take place at a time which have the maximum resemblance. The resemblance matrix is updated after each merger and the process is continued till desired number of groups is left. A C-scan image based on the cluster analysis output, thus, not only gives types of zones in the plates but also their spread. The generated images are then used for fractal analysis.

IV. Algorithm to Find Fractal Dimension of A 2-D Digitized Image

The algorithm discussed in this section is used for estimation of the fractal dimension of a 2-D digitized image as proposed by Bhatt et al. [6]. Any N by N 2-D digitized image, as shown in Fig. 1, containing N^2 pixels is considered. A rectangular domain having different pixels in two directions is also possible to be considered by the algorithm.

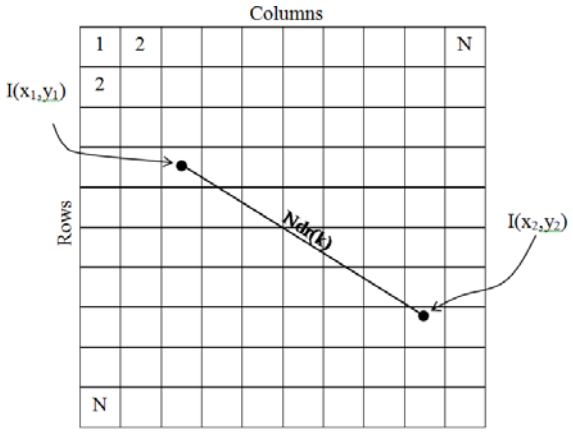

Fig. 1 Schematic diagram of the N by N 2-D digitized image

Here I(x,y) represents the intensity value of any such pixel with coordinate x,y. The fractal graph of any such image is visualized as the plot of log (NMSID) vs. log (NSR). As before, the NSR corresponds to the normalized scale range vector and corresponds to the possible Euclidean distances between any pair of pixel in the concerned image. Thus

$$NSR = [ndr(1), ndr(2), ..., ndr(k), ..., ndr(m)] \quad (1)$$

where,

$$ndr(k) \le \left[(x_2 - x_1)^2 + (y_2 - y_1)^2\right]^{1/2} < ndr(k+1) \quad (2)$$

The NMSID vector consists of different absolute-intensity difference averages around each normalized reference scale (NSR), i.e.,

$$NMSID = [ndi(1), ndi(2), ..., ndi(k), ...ndi(m)] \quad (3)$$

where,

$$ndi(k) = \frac{\sum_{x_1=1}^{N}\sum_{y_1=1}^{N}\sum_{x_2=1}^{N}\sum_{y_2=1}^{N}\left|I(x_2,y_2) - I(x_1,y_1)\right|}{npn(k)} \quad (4)$$

Here *npn* is the normalized pixel pair number vector, which consists of elements that represent the number of pixel pairs with scale (distance) values similar to the reference scale. Plotting log (NMSID) vs. log (NSR) for I=1, 2… m, results in a curve consisting of m points which is the fractal graph of the corresponding image. For a practical digitized image, the fractal graph initially rises up to certain NSR showing the fractal nature and thereafter it dips. A linear fractal graph represents a perfect fractal; otherwise a least square linear regression on the relevant portion of it gives the required slope b. Fractal dimension FD of the digitized image is then calculated from the relation $FD = 3 - b$.

The significance of the above relation can be illustrated as follows. The initiator in this case is a three-dimensional (3D) cube. It can be represented in terms of cubic voxels of size, say, ε. Now if the volume of the cube is unity, then N_ε the number of voxels in the cube, is given by

$$N_\varepsilon = \left(\frac{1}{\varepsilon}\right)^3 \quad (5)$$

However, if the cube surface is not perfect, i.e., it has dents in it, then the number of voxels contained in the cube will be less than N_ε, given by

$$N_\varepsilon = \left(\frac{1}{\varepsilon}\right)^n \quad (6)$$

where n<3. This number n is the fractal dimension.

Thus any 2-D digitized image can be represented as a fractal having a fractal dimension between 2 and 3 while an image with constant intensity is similar to a cube with no dents and its fractal dimension will be 3 as per definition. Moreover, it is important to note that the FD, evaluated as above, will vary since the slope of the best linear fit depends on the range-of- scales of distances being selected. It is a common practice to consider the range of NSR in which the fractal graph exhibits nearly linear behaviour.

V. Fractal Dimension of A 2-D Digitized Image

In this section generation of the fractal graph of a 2-D Digitized image, and the FD of the image computed thereof are presented. Figures 2 - 5 show the digitized image of a 10 mm and 15mm Kevlar epoxy composite plate impacted at different striking velocity.

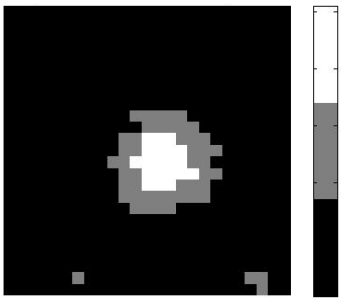

Fig. 2 Peak amplitude based 2-D Image of 10mm Kevlar-epoxy composite plate impacted with a striking velocity of 360.8m/sec

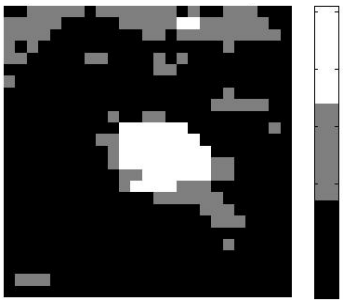

Fig. 3 Peak amplitude based 2-D Image of 10mm Kevlar-epoxy composite plate impacted with a striking velocity of 253.7m/sec

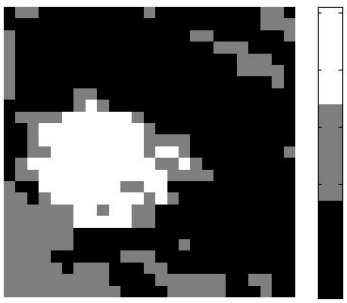

Fig. 4 Peak amplitude based 2-D Image of 15mm Kevlar-epoxy composite plate impacted with a striking velocity of 350.1m/sec

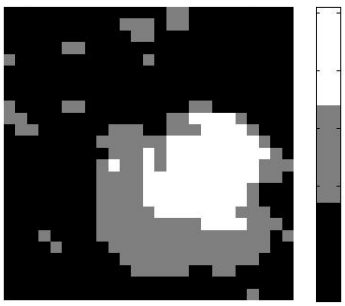

Fig. 5: Peak amplitude based 2-D Image of 15mm Kevlar-epoxy composite plate impacted with a striking velocity of 225.1.1m/sec

In all the cases the images contain $25^2 = 625$ pixels. As per the algorithm outlined in section 4 the fractal graphs of the images are visualized as the plot of log (NMSID) vs. log (NSR). It is evident from the plot that the entire ranges in the NSR do not exhibit the fractal behavior. Therefore, it is truncated at a suitable point up to which the curves exhibit a fractal nature. The truncated fractal graphs with respective best-fit lines in the least square sense are shown in Figs. 6 - 9.

Corresponding slopes (b) of the best-fit lines are calculated and are shown in respective figures. The fractal dimension FD is then calculated from the relation FD = (3-b). The values of FD for the 2D images shown in Figs. 2 through 5 are 2.17282, 2.13877, 2.22114 and 2.203223 respectively. These FDs are not so different and it is expected since the corresponding images have the similar intensity of roughness (each has a distinct defect zone). This is reflected in the calculated values of the FD.

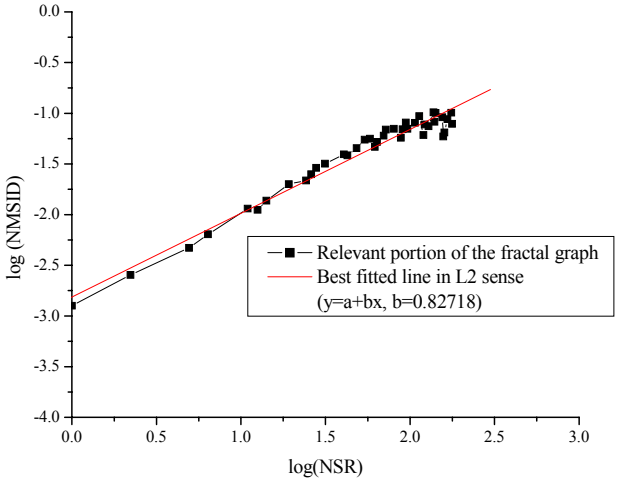

Fig. 6 Fractal graph of peak amplitude based 2-D Image (10mm Kevlar epoxy composite plate impacted with a striking velocity of 360.8m/sec)

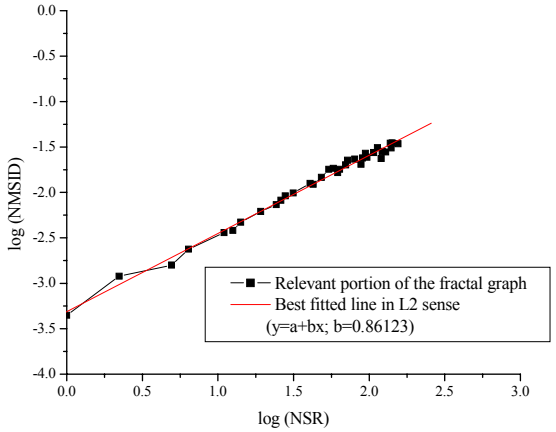

Fig. 7 Fractal graph of peak amplitude based 2-D Image (10mm Kevlar epoxy composite plate impacted with a striking velocity of 253.7m/sec)

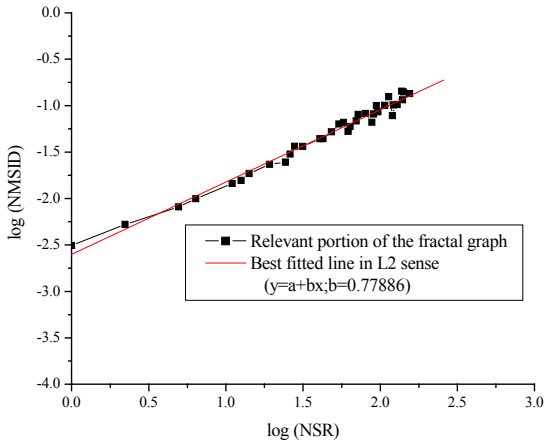

Fig. 8 Fractal graph of peak amplitude based 2-D Image (15mm Kevlar Polypropylene composite plate impacted with a striking velocity of 350.1m/sec)

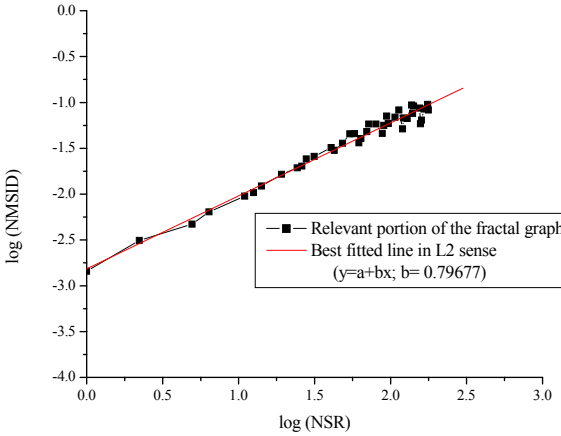

Fig. 9 Fractal graph of peak amplitude based 2-D Image (15mm Kevlar Polypropylene composite plate impacted with a striking velocity of 225.1m/sec)

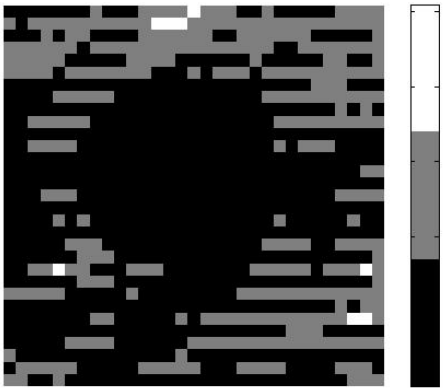

Fig. 10 Peak amplitude based 2-D Image of Glass-epoxy composite with Teflon insert

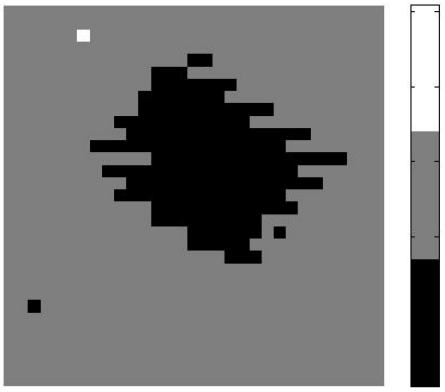

Fig. 11 Shannon entropy based 2-D Image of Glass-epoxy composite with Teflon insert

The utility of obtaining the FD of a C-scan image may be more relevant when many panels or test blocks are tested/scanned and then imaged. It may not be out of context to determine the FD of the image in identifying the existence of a distinct different region. FD is capable to make such distinctions effectively. Such identification will help the user to be careful with those regions for which the FD has a lower value. To demonstrate this capability, two other digitized images of the glass epoxy composite panel with the Teflon insert, shown in Figs. 10 and 11, are considered. The image, shown in Fig. 11, shows a distinct Teflon inclusion (i.e., more roughness) while the other one shows it blurredly, as if, there is no inclusion (less roughness).

Both the images contain 31^2=961 pixels. Based on the algorithm the fractal graph has been generated. The truncated fractal graphs (up to the point it exhibits a fractal nature) and the respective best fit lines in the least square sense are shown in Figs 12 and 13 respectively. The values of FD for the above cases are found to be 2.85135 and 2.11972 respectively. These values are sharply different showing FD as a true indicator of roughness in a digitized image. This is to say that in absence of no distinct zone in an image, its roughness will fall, leading to a flatter fractal graph and resulting in a higher FD. When such pixels are clustered around a zone in the image, the region becomes distinct causing an increase in roughness of the image. Such a distinct existence is reflected in the quantitative value of the FD. This may augment the automated procedure of a C-scan image generation and its subsequent evaluation.

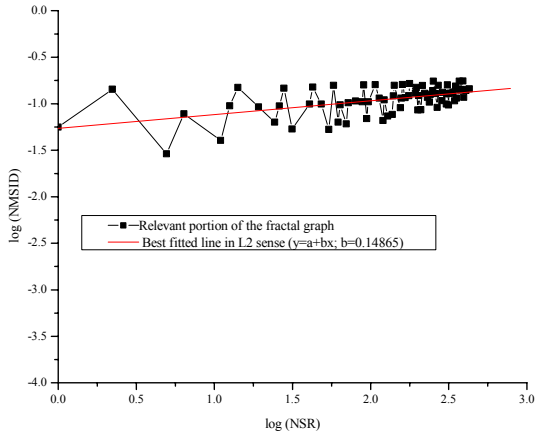

Fig. 12 Fractal graph of peak amplitude based 2-D Image (Glass-epoxy composite with inclusion Insert)

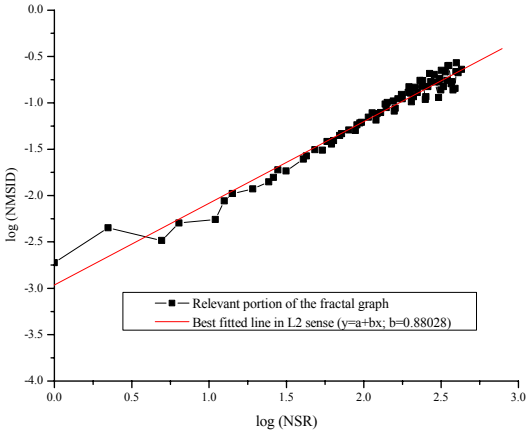

Fig. 13 Fractal graph of Shannon entropy based 2-D Image (Glass-epoxy composite with inclusion Insert)

VI. Conclusions

An automated way of identifying existence of a damage zone in an image is conceived. When large number of panels is tested, each of them may not contain damage. An automated way of differentiating them is implemented in this research. This is accomplished through fractal analysis. An algorithm for evaluation of fractal dimension of any 2-D digitized image is implemented by developing a computer code. Fractal analysis of C-scan images reveals that FDs can automatically differentiate existence of a flawed zone in an image from an image having no flaw. Such analysis may further augment automated inspection.

References

[1] B. B. Mandelbrot, and J. W. Wallis, "Fractional Brownian Motions," *Fractional Noises and Applications*, *SIAM review*, 10: 422-437, 1968.
[2] B. B. Mandelbrot, "The Fractal Geometry of Nature," W. H. Freeman, San Francisco, CA, 1982.
[3] A. P. Pentland, "Shading into Texture," *Artificial Intelligence*, 29:147-170, 1986.
[4] T. Lundhal, W. J. Ohley, S. M. Kay, and R. Siffert, "Fractional Brownian motion: A Maximum Likehood Estimator and Its Application to Image Texture," *IEEE transactions on Medical Imaging*, 5:152-161, 1986.
[5] C. C. Chen, J. S. Deponte, and M. D. Fox, "Fractal Feature Analysis and Classification in Medical Imaging," *IEEE transactions on Medical Imaging*, 8:133-142, 1989.
[6] V. Bhatt, P. Munshi, and J. J. Bhattacharjee, "Application of Fractal Dimension for Nondestructive Testing," *Materials Evaluation*, 49:1414-1418, 1991.
[7] P. Munshi, M. Maisl, and H. Reiter, "Quantitative Assessment of Radiographic Images Using Region-of-Interest Fractal Graphs," *Nondestructive Testing and Evaluation*, 11:33-42, 1994.
[8] P. Munshi, M. Maisl, and H. Reiter, "A New Method of Characterizing Patterns in X-ray Tomographic Images of a Composite Specimen," *Nuclear Instruments and Methods in Physics Research Section B: Beam Interactions with Materials and Atoms*, 108:205-212, 1996.
[9] C. E. Shannon, and W. Weaver, "The Mathematical Theory of Communication," *Univ. Illinois press. Chicago*, 1963.
[10] PCUS11 Ultrasonic P/R Board Manual, Doc # EBD003-1, *Fraunhoffer Institute for Non-Destructive Testing*, Saarbruecken, Germany, 1999.
[11] QUT Ultrasonic testing software Manual, Version 4, *Quality Network (QNET) Pvt. Ltd*, 1999.
[12] H. Charles Romesburg, "Cluster Analysis for Researchers," *Lulu Press*, North Carolina, United States of America, 2004.